An Inhibitory Antibody Blocks the First Step in the Dithiol/Disulfide Relay Mechanism of the Enzyme QSOX1

ARTICLE *in* JOURNAL OF MOLECULAR BIOLOGY · JULY 2013

Impact Factor: 4.33 · DOI: 10.1016/j.jmb.2013.07.011 · Source: PubMed

4 AUTHORS, INCLUDING:

Iris Grossman
Weizmann Institute of Science
6 PUBLICATIONS **62** CITATIONS
SEE PROFILE

Assaf Alon
Whitehead Institute for Biomedical Research
12 PUBLICATIONS **245** CITATIONS
SEE PROFILE

Tal Ilani
Weizmann Institute of Science
14 PUBLICATIONS **510** CITATIONS
SEE PROFILE

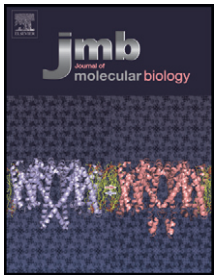

An Inhibitory Antibody Blocks the First Step in the Dithiol/Disulfide Relay Mechanism of the Enzyme QSOX1

Iris Grossman, Assaf Alon, Tal Ilani and Deborah Fass

Department of Structural Biology, *Weizmann Institute of Science, Rehovot 76100, Israel*

Correspondence to Deborah Fass: *deborah.fass@weizmann.ac.il*
http://dx.doi.org/10.1016/j.jmb.2013.07.011
Edited by S. Sidhu

Abstract

Quiescin sulfhydryl oxidase 1 (QSOX1) is a catalyst of disulfide bond formation that undergoes regulated secretion from fibroblasts and is over-produced in adenocarcinomas and other cancers. We have recently shown that QSOX1 is required for incorporation of particular laminin isoforms into the extracellular matrix (ECM) of cultured fibroblasts and, as a consequence, for tumor cell adhesion to and penetration of the ECM. The known role of laminins in integrin-mediated cell survival and motility suggests that controlling QSOX1 activity may provide a novel means of combating metastatic disease. With this motivation, we developed a monoclonal antibody that inhibits the activity of human QSOX1. Here, we present the biochemical and structural characterization of this antibody and demonstrate that it is a tight-binding inhibitor that blocks one of the redox-active sites in the enzyme, but not the site at which de novo disulfides are generated catalytically. Sulfhydryl oxidase activity is thus prevented without direct binding of the sulfhydryl oxidase domain, confirming the model for the interdomain QSOX1 electron transfer mechanism originally surmised based on mutagenesis and protein dissection. In addition, we developed a single-chain variant of the antibody and show that it is a potent QSOX1 inhibitor. The QSOX1 inhibitory antibody will be a valuable tool in studying the role of ECM composition and architecture in cell migration, and the recombinant version may be further developed for potential therapeutic applications based on manipulation of the tumor microenvironment.

Introduction

Quiescin sulfhydryl oxidase 1 (QSOX1) is a disulfide catalyst that uses a bound flavin adenine dinucleotide (FAD) cofactor to mediate transfer of electrons from pairs of thiol groups to molecular oxygen, generating hydrogen peroxide as a by-product [1]. QSOX1 shares this fundamental catalytic activity of disulfide formation with a number of other enzymes that function in early-stage protein folding in the endoplasmic reticulum (ER) [2] and with enzymes that mediate folding and retention of proteins in the mitochondrial intermembrane space [3]. However, QSOX1 is the only disulfide catalyst known to be localized primarily to organelles downstream of the ER in the secretory pathway and to undergo regulated secretion from certain cells [4]. The presence of a conserved disulfide catalyst in environments containing proteins that typically bear their full complement of disulfides, having already been exposed to the oxidative and quality control mechanisms in the ER, suggests that as yet undiscovered pathways of protein modification, refolding, and assembly exist in post-ER compartments.

Although direct substrates of QSOX1 remain to be experimentally identified, we have shown that QSOX1 is required for proper assembly of extracellular matrix (ECM) resembling the basement membrane (BM) in cell culture [5]. BM is the layer of ECM at the interface between body cavities or blood vessels and underlying stromal fibroblasts, and many BM components are produced by fibroblasts. BM components include laminin, collagen IV, heparin sulfate proteoglycans, entactin, and many other contributing macromolecules [6]. BM is a complex medium for cell adherence and signaling, and its composition and properties influence the behavior of associated epithelial cells.

The BM component most notably affected by QSOX1 is laminin [5]. We observed that depletion of QSOX1 led to the appearance of soluble laminin isoforms in the supernatants of confluent fibroblast cultures, whereas laminin was incorporated into the

insoluble ECM material under normal conditions. We further observed that BM produced in the absence of QSOX1 failed to support adherence and migration of tumor epithelial cells introduced to the fibroblast layer. Laminin isoforms most sensitive to the presence of QSOX1 in these co-culture assays, that is, those containing the α4 chain, have been shown previously to contribute to the migratory activity of leukemia and lymphoma cells [7] and to the progression of glioblastoma [8]. The laminin α4 chain is a biomarker for or associated with tumor invasion in many other cancers as well [9–14].

QSOX1 is a multi-domain protein that undergoes a series of dithiol/disulfide exchange steps to pass electrons from substrate thiols to its FAD cofactor [15]. The two main redox-active domains of the enzyme, the amino terminus of which interacts with the thiol-containing substrates and the carboxy terminus of which catalyzes reduction of molecular oxygen, are proposed to change their relative orientations during the reaction cycle. In particular, the redox-active di-cysteine motif in the amino-terminal, thioredoxin-fold domain (Trx1) (Fig. 1a) must be sufficiently solvent exposed to accept electrons from substrate proteins. The Trx1 domain then buries itself against the redox-active di-cysteine motif of the disulfide-generating Erv-fold (Erv) domain to transfer the electrons further (Fig. 1b). A set of crystal structures of QSOX enzymes illustrated the nature of these conformational changes and identified the flexible linker that permits such rearrangements [16].

A number of considerations suggest that inhibitory antibodies would be an excellent strategy for controlling QSOX1 activity for research and therapeutic purposes. The requirement for large conformational changes and domain–domain interactions suggests that QSOX1 presents an expanded target for inhibition by binding compared to other enzymes. In addition, considering that the role of QSOX1 in BM assembly is executed extracellularly, cell penetrability is not an obligatory characteristic of an inhibitor. Monoclonal antibody therapy is becoming increasingly popular in cancer treatment, mainly because of the high affinity and specificity that antibodies offer [17]. Several monoclonal antibodies have been approved as drugs for various cancers [18], and antibodies represent a third of the proteins under clinical trials in the USA [17,19]. We therefore generated with hybridoma

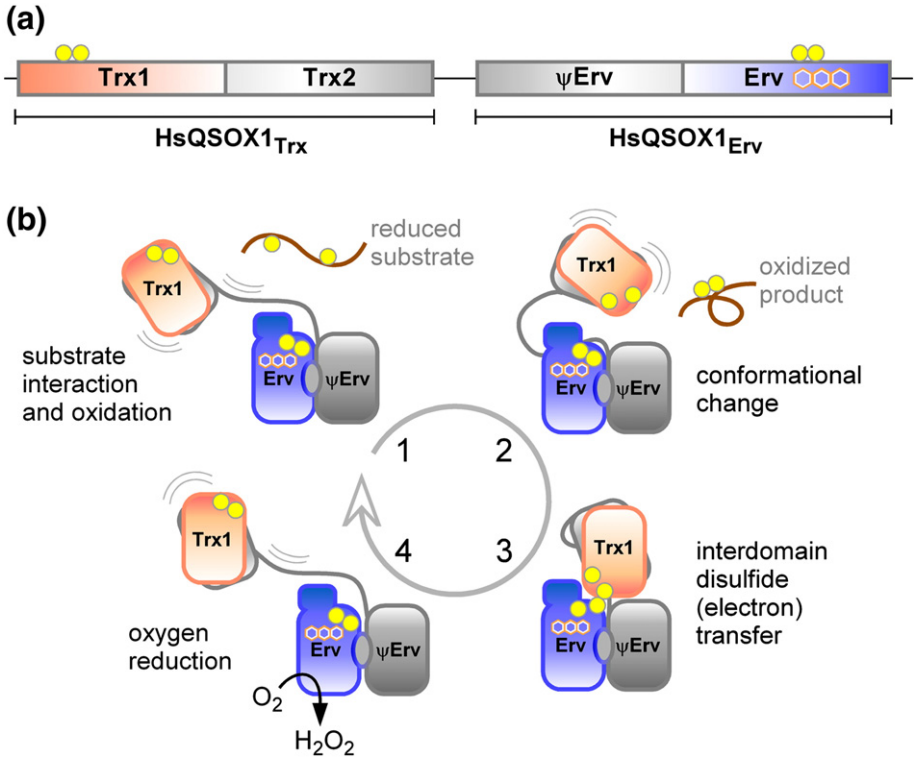

Fig. 1. Domain organization and reaction cycle of human QSOX1 (HsQSOX1). (a) Schematic diagram of the four domains of HsQSOX1. The amino-terminal fragment, $HsQSOX1_{Trx}$, is composed of two Trx-fold domains. The carboxy-terminal fragment, $HsQSOX1_{Erv}$, is composed of two Erv-fold domains. The degenerate Erv-like sulfhydryl oxidase domain that has lost its active-site cysteines and cofactor binding capability is designated as "ψErv". Paired yellow balls represent CXXC motifs (redox-active disulfides). The three fused hexagons indicate the FAD cofactor, bound by the Erv domain. (b) Steps in the reaction cycle of substrate oxidation and oxygen reduction by HsQSOX1. Domains are represented with the same names and colors as in (a), with a gray line representing the linker between the Trx2 domain and the ψErv domain. Fused yellow balls represent disulfide bonds. Separated yellow balls indicate reduced cysteines.

technology a monoclonal antibody inhibitor of QSOX1 and used it to confirm the role of QSOX1 in incorporation of laminin into the ECM [5].

In this study, we have characterized the structure and mechanism of the anti-QSOX1 monoclonal antibody inhibitor, MAb492.1. Determination of the antibody binding site on the QSOX1 enzyme validates the working model for the QSOX1 catalytic cycle and confirms the essential role of an interdomain relay in delivering dithiol-derived electrons to the site of de novo disulfide generation. In addition, a demonstration that inhibitory activity is recapitulated by a recombinant, single-chain version of the antibody opens the door to further engineering of the reagent for medical and biotechnological applications.

Results

Determination of the inhibitory constant of MAb492.1

The sulfhydryl oxidase activity of QSOX1 secreted from confluent fibroblasts was blocked by 250 nM MAb492.1 in a previous study [5]. To quantify inhibition more precisely, we tested a range of antibody concentrations against recombinant human QSOX1 (hereafter referred to as HsQSOX1) in an assay of oxidation of the model substrate reduced and denatured RNase A (rdRNase). In each case (Fig. 2a and Supplementary Fig. 1), IC_{50} values closely approximating the enzyme concentrations used in the assays were observed, suggesting near-stoichiometric binding of HsQSOX1 by MAb492.1 and effective inhibition *in vitro*.

To provide a measure of the actual K_i of the inhibitor, lower enzyme and antibody concentrations were needed than were practical in the rdRNase assay. To achieve these concentrations, we used an oxygen consumption assay, which monitors the rate of decrease of dissolved oxygen as it is reduced by HsQSOX1 to hydrogen peroxide. Furthermore, this assay allows direct determination of initial rates and not merely degree of activity. A strong reducing agent, dithiothreitol (DTT), was used as an electron donor in this experiment at a concentration that preserves antibody integrity (Supplementary Fig. 2). Reaction rates were calculated from experiments using 25 nM HsQSOX1 and various concentrations of MAb492.1. Fitting the results to a model for a tight-binding inhibitor [20,21] yielded an apparent inhibitory constant (K_i) of 0.9 ± 0.1 nM (Fig. 2b). As demonstrated below, MAb492.1 blocks access to the Trx1 domain redox-active site. Under the assumption that the primary route for reduction of the sulfhydryl oxidase active site in the Erv domain is by delivery of electrons from the Trx1 domain, MAb492.1 is expected to be a competitive inhibitor.

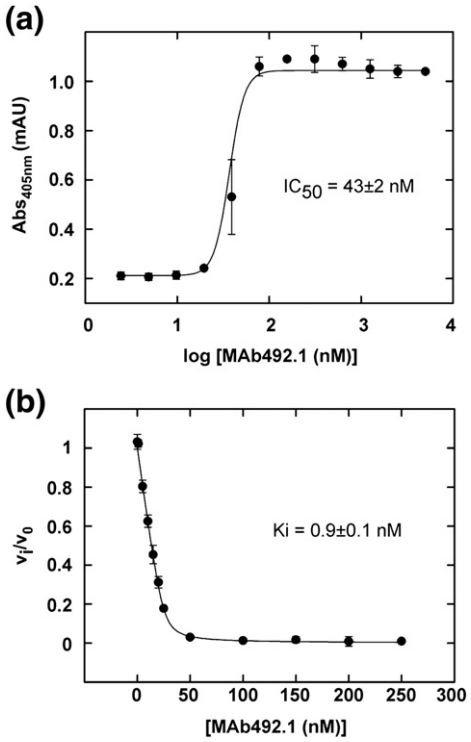

Fig. 2. Determination of inhibition constant for MAb492.1 (a) Dose–response curve of MAb492.1 to 50 nM HsQSOX1, based on results from a colorimetric assay quantifying rdRNase oxidation. The inhibitory activity is expressed as absorbance at 405 nm, representing the free thiols that reacted with DTNB. Three measurements were made for each MAb492.1 concentration and averaged. Error bars represent standard deviation. The IC_{50} was determined by nonlinear regression analysis and yielded a value of 43 ± 2 nM. (b) Inhibition curve of MAb492.1 to 25 nM HsQSOX1, based on results from oxygen electrode assays at different MAb492.1 concentrations (ranging from 1 nM to 250 nM). The inhibitory activity is expressed as the ratio of the inhibited rate to the uninhibited rate (v_i/v_0). Three measurements were made for each MAb492.1 concentration and averaged. Error bars represent standard deviation. The inhibition constant was determined by nonlinear regression analysis and yielded a K_i value of 0.9 ± 0.1 nM.

Reaction rates in the presence of competitive inhibitors typically vary with substrate concentration, and thus the apparent K_i does not necessarily represent the actual K_i. Nevertheless, we observed that MAb492.1 inhibition is independent of substrate concentration (Supplementary Fig. 3), implying that the dissociation of the complex between MAb492.1 and HsQSOX1 is slow on the timescale of the experiment and is not induced by substrate [21,22]. Under these conditions, the apparent K_i becomes the actual K_i.

Following the *in vitro* determination of the inhibitory constant, inhibition was quantified in cell culture assays based on the activity of HsQSOX1 in ECM assembly.

HsQSOX1 affects laminin incorporation into the ECM produced by fibroblasts, which in turn affects the ability of epithelial cells to adhere to and migrate through the fibroblast monolayer [5]. Therefore, quantification of epithelial cell adhesion and migration provides an indirect readout for HsQSOX1 physiological activity.

For adhesion assays, fibroblast cultures were grown for 4 days in the presence of various concentrations of MAb492.1. During this time, about 40 nM secreted QSOX1 is expected to accumulate in the culture supernatant [5]. Fluorescently labeled epithelial cells were then added in fresh medium to the mature fibroblast culture and incubated for 3 h. Non-adherent epithelial cells were washed away, and adherent cells were counted. This assay gave a midpoint for inhibition of epithelial cell adherence at approximately 125 nM MAb492.1 (Fig. 3a). As a negative control, an unrelated antibody for β actin supplied to the growing fibroblasts showed no subsequent effect on adherent cell numbers (Fig. 3b). As a positive control, blocking of the laminin receptor α6 integrin on the epithelial cells resulted in a decrease in adherent cell numbers (Fig. 3b).

For migration assays, fibroblast monolayers were first grown for 4 days on the porous base of a culture insert in the presence of various concentrations of MAb492.1. Fluorescently labeled tumor cells were then added to the confluent fibroblast layer, and labeled cells that crossed the monolayer and penetrated the porous membrane by 24 h were counted. The midpoint for epithelial cell migration occurred at a MAb492.1 concentration of about 150 nM in this experiment (Fig. 3c). Together, these results indicate that MAb492.1 is a potent inhibitor of physiological HsQSOX1 activity. Importantly, comparing the effective IC_{50} values in cell culture with the known K_i suggests that suitable MAb492.1 dosages for some biological applications may depend on the absolute amount of HsQSOX1 present and the accessibility of the enzyme, rather than on the intrinsic binding and inhibition constants of the antibody.

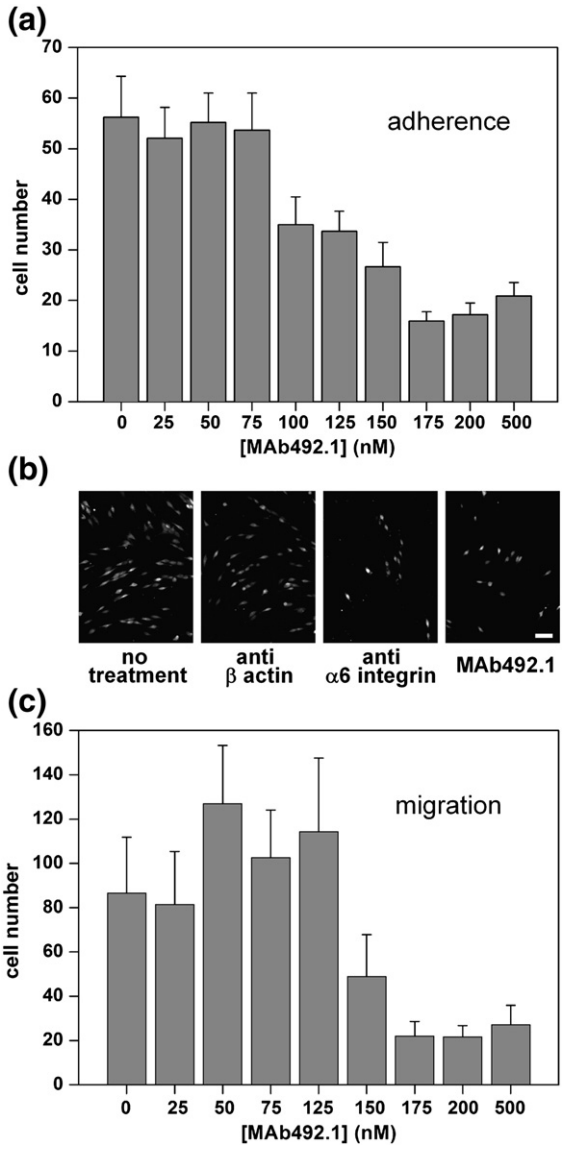

Fig. 3. Inhibition of tumor cell adhesion and migration by MAb492.1. (a) Quantification of adhesion of fluorescently labeled epithelial cells to a fibroblast monolayer grown in the presence of various concentrations of MAb492.1. The average number of adherent epithelial cells per field is reported for each antibody concentration. Error bars are standard error of the mean. (b) Representative fields of adherent epithelial cells from experimental and control samples are presented. MAb492.1 and anti-actin were applied to the fibroblasts, whereas anti-α6 integrin was applied to the tumor epithelial cells. The scale bar represents 100 μm. (c) Quantification of migration of fluorescently labeled epithelial cells through a fibroblast monolayer grown in the presence of various concentrations of MAb492.1. The average number of labeled cells having passed through the fibroblast layer and the porous filter support of the assay chamber is reported for each antibody concentration. Error bars are standard error of the mean.

Sequencing of the MAb492.1 antibody clone

The sequence of MAb492.1 was determined by reverse-transcription and polymerase chain reaction (PCR) from the hybridoma clone. The variable region of the light chain was amplified with a small set of degenerate primers [23]. In contrast, the variable region of the heavy chain could not be amplified using a comparable primer mix, consistent with the relative difficulty of amplifying heavy chains observed previously [24]. Therefore, the MAb492.1 heavy chain was amplified using optimized primers for mouse single-chain variable fragment (scFv) repertoire cloning [25]. Each amplified fragment was cloned into the pGEM-T Easy vector and sequenced. These sequences (Table 1) were analyzed using tools associated with the ImMuno-

GeneTics database [26] and were confirmed to be productively rearranged sequences. The variable regions showed over 94% identity to database entries for variable regions of antibodies produced in mice. The sequences were also confirmed by liquid chromatography–tandem mass spectrometry (LC–MS/MS) of purified MAb492.1 (Table 1).

Determination of the antibody binding site on HsQSOX1

It was previously observed that limited proteolysis of avian QSOX1 produces two stable fragments [27]. Similar observations were made for mammalian QSOX1 enzymes, and the structures of the two fragments of human QSOX1, $HsQSOX1_{Trx}$ and $HsQSOX1_{Erv}$ (Fig. 1a), were solved using X-ray crystallography [16,28]. To determine whether the binding site for MAb492.1 resides in $HsQSOX1_{Trx}$ or $HsQSOX1_{Erv}$, we produced each of the fragments in bacteria and performed two complementary binding assays. In the first assay, binding of MAb492.1 to $HsQSOX1_{Trx}$ or $HsQSOX1_{Erv}$ was compared with binding to full-length HsQSOX1 by enzyme-linked immunosorbent assay (ELISA). $HsQSOX1_{Trx}$, containing the Trx1 and Trx2 domains, bound MAb492.1 to the same extent as did full-length HsQSOX1 (Fig. 4a). $HsQSOX1_{Erv}$, on the other hand, did not bind MAb492.1 at any concentration tested. The second binding assay used size-exclusion chromatography. The elution profiles of HsQSOX1, $HsQSOX1_{Trx}$, and $HsQSOX1_{Erv}$ were measured in the presence and absence of MAb492.1. Elution of both HsQSOX1 and $HsQSOX1_{Trx}$ was shifted to larger apparent molecular weights following incubation with MAb492.1, but elution of $HsQSOX1_{Erv}$ was unaffected (Fig. 4b), confirming that MAb492.1 binds to the amino-terminal portion of HsQSOX1. Furthermore, binding was not prevented by reduction of the active-site disulfide of $HsQSOX1_{Trx}$ (Supplementary Fig. 4). The finding that MAb492.1 binds the oxidoreductase module rather than the sulfhydryl oxidase module of HsQSOX1 is noteworthy, as the antibody is a potent inhibitor of HsQSOX1 sulfhydryl oxidase activity.

Table 1. MAb492.1 variable region amino acid sequences

Sequence				Chain
DVVMTQTHKFMSTSVGDRVSITCKASQDVSTAVAWYQQKSGQSPKLLIHSAS YRYTGVPDRFTGSGSGTDFTFTISSVQAEDLAVYYCQQHYSIPLTFGAGTKLELK				light
QVQLKQSGPGLVAPSQSLSITCTVSGFSLTGYGVNWVRQSPGKGLEWLGMIWGDGRTD YKSALKSRLSITKDNSKSQVFLKMNSLQTDDTARYFCASDYYGSGSFAYWGQGTLVTVSA				heavy
MW (calc)	MW (exp)	Peptide	Enzyme	
2037.9612	2037.9634	DVVMTQTHKFMSTSVGDR	trypsin	light
2742.3140	2742.3148	DVVMTQTHKFMSTSVGDRVSTICK		
1686.8069	1686.8076	FMSTSVGDRVSITCK		
1680.8107	1680.8110	ASQDVSTAVAWYQQK		
1058.5873	1058.5880	LLIHSASYR		
1766.8332	1766.8344	DVVMTQTHKFMSTSVG	chymotrypsin/ Asp-N	
1841.8612	1841.8642	MSTSVGDRVSITCKASQ		
1870.9901	1870.9938	QQKSGQSPKLLIHSASY		
1075.4459	1075.4468	TGSGSGTDFTF		
1203.6863	1203.6886	SIPLTFGAGTKL		
1985.9782	1985.9824	QSPGKGLEWLGMIWGDGR	trypsin	heavy
1488.7184	1488.7206	GLEWLGMIWGDGR		
1995.9513	1995.9510	GLEWLGMIWGDGRTDYK		
1250.5561	1250.5576	MNSLQTDDTAR		
995.4713	995.4732	SLTGYGVNW	chymotrypsin/ Asp-N	
1711.8794	1711.8808	GVNWVRQSPGKGLEW		
1179.6611	1179.6637	DYKSALKSRL		
1837.0057	1837.0096	KSRLSITKDNSKSQVF		

The table displays representative peptides detected by LC–MS/MS.

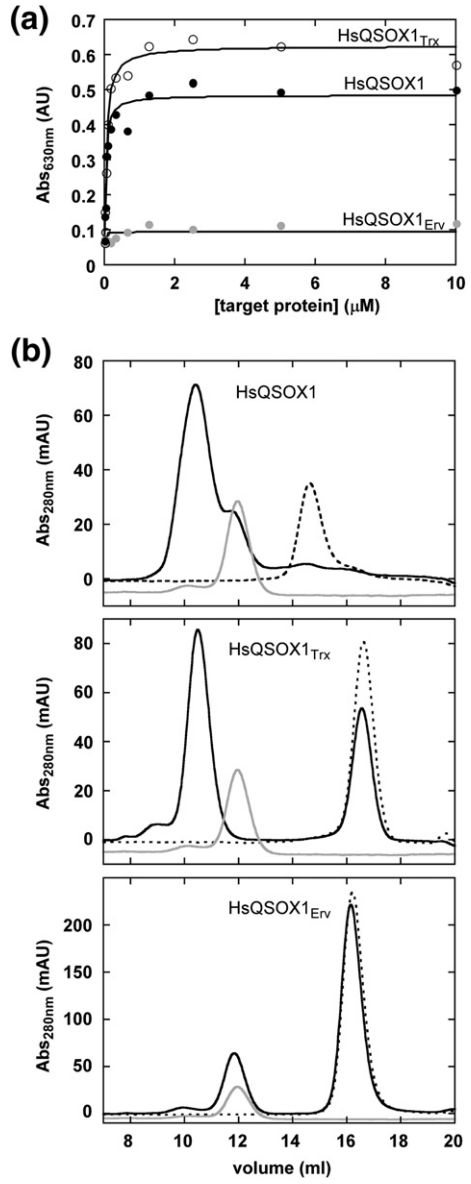

Fig. 4. MAb492.1 binds the HsQSOX1 amino-terminal fragment, HsQSOX1$_{Trx}$. (a) Binding curves of MAb492.1 to full-length HsQSOX1, and to its two fragments, based on ELISA. High absorbance at 630 nm achieved at low target protein concentrations indicates tight binding. (b) Analytical size-exclusion chromatography. Gray lines represent the elution profile of MAb492.1 alone. Broken lines represent the elution profile of HsQSOX1, or one of its fragments, alone. Black lines represent the elution profiles of mixtures of MAb492.1 and HsQSOX1 or a fragment thereof.

Structure of a complex between inhibitor and HsQSOX1

To determine how MAb492.1 blocks HsQSOX1 sulfhydryl oxidase activity, we characterized the interaction between the MAb and the enzyme using X-ray crystallography. A Fab fragment derived from MAb492.1 (Fab492.1) was prepared by papain digestion for co-crystallization with HsQSOX1$_{Trx}$. The tight binding and inhibition of HsQSOX1 by the Fab were verified using the rdRNase oxidation assay (Supplementary Fig. 5).

Table 2. Data collection and refinement statistics for the Fab492.1–HsQSOX1$_{Trx}$ complex

	Fab492.1–HsQSOX1$_{Trx}$
Data collection	
Space group	$P6_1$
Resolution (Å)	50–2.70 (2.75–2.70)
Unique reflections	38,606
Cell dimensions	
a, *b*, *c* (Å)	209.31, 209.31, 55.27
α, β, γ (°)	90, 90, 120
R_{sym}	0.092 (0.363)
$I/\sigma I$	14.4 (2.0)
Completeness (%)	97.3 (91.9)
Redundancy	5.1 (3.8)
Refinement	
Resolution (Å)	50–2.70
Number of reflections: working/test set	34,719/2622
R_{work}/R_{free}	0.202/0.237
Number of atoms	
Protein	5152
Phosphate	10
Water	337
Mean *B*-factors	37.0
Fab492.1	40.4
HsQSOX1$_{Trx}$	30.4
Solvent	38.8
RMSD	
Bond lengths (Å)	0.006
Bond angles (°)	1.44
Ramachandran (%)	
Preferred regions	95.5
Additional allowed regions	4.5
Disallowed regions	0

Values in parentheses are for the highest-resolution shell.

The structure of the complex between HsQSOX1$_{Trx}$ and Fab492.1 was determined to 2.7 Å resolution (Table 2). The crystal structure revealed that Fab492.1 recognizes the Trx1 domain (Fig. 5a). In particular, Fab492.1 binds the active site, burying the CXXC motif and a large surface area surrounding it. The interface area was calculated [29] to be 948.7 Å^2. All six complementarity-determining regions (CDRs) participate in binding (Fig. 5b). The heavy chain is responsible for most of the interactions (Fig. 6b and Supplementary Table 1), including burial of the CXXC motif using all three CDRs. The light chain, responsible for 40% of the complex interface (407.6 Å^2), binds a large surface area away from the active site but continuous with the surface occluded by the heavy chain (Fig. 5c). The light chain binds Trx1 through hydrophobic interactions and a network of hydrogen bonds (Fig. 6a and Supplementary Table 1), presumably stabilizing the orientation of the heavy chain relative to the active site. The structure of complexed HsQSOX1$_{Trx}$ shows few deviations from the structure

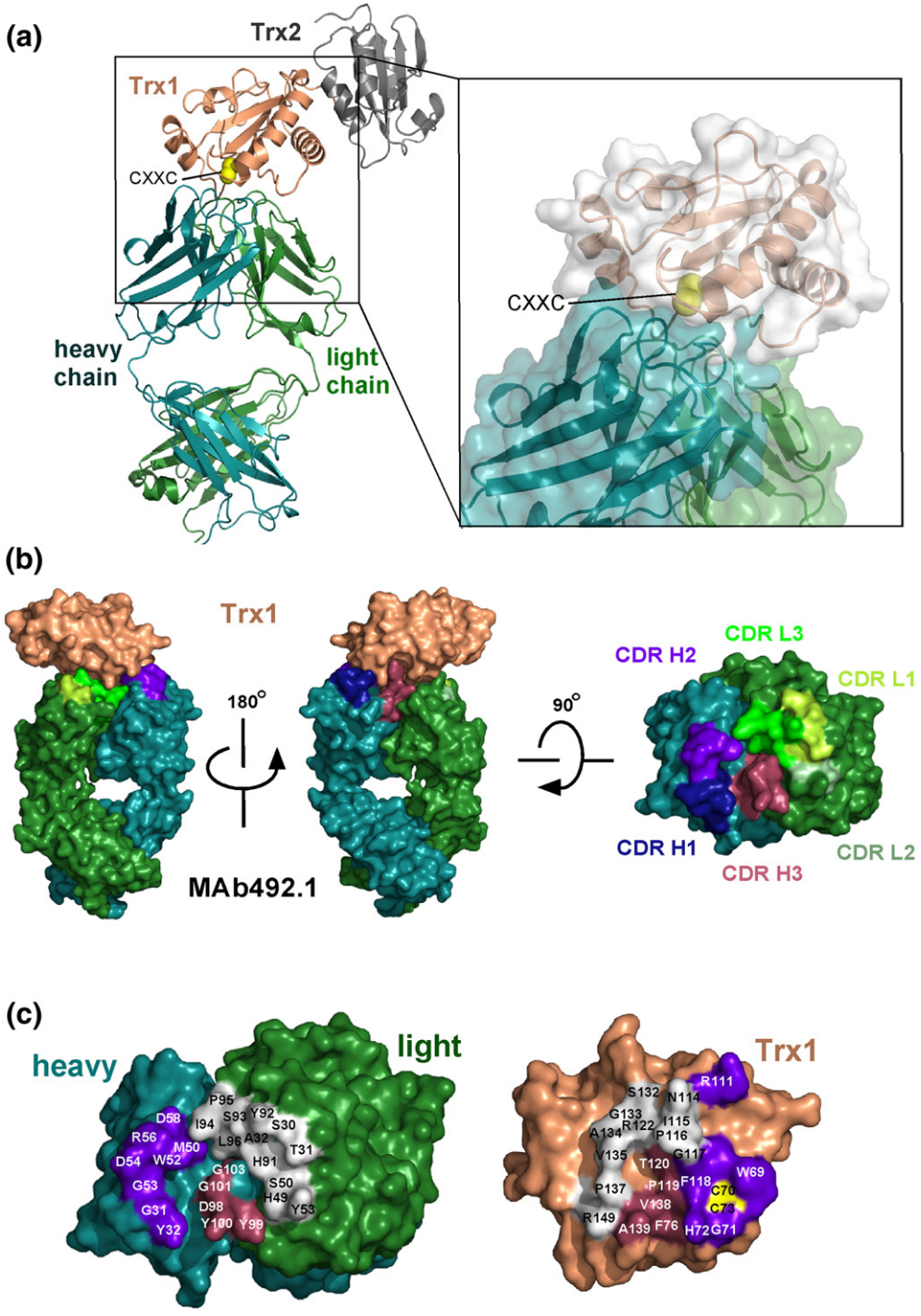

Fig. 5. Structure of the Fab492.1–HsQSOX1$_{Trx}$ complex. (a) Structure of the complex between HsQSOX1$_{Trx}$ (Trx1, peach; Trx2, gray; CXXC motif sulfurs, yellow spheres) and Fab492.1 (heavy chain, blue; light chain, green). The redox-active CXXC motif in the HsQSOX1 Trx1 domain is buried in the interface. (b) Surface representation of the Fab492.1–HsQSOX1$_{Trx}$ complex highlighting the CDRs. In the right view, showing Fab492.1 alone, the CDRs are labeled in corresponding colors. (c) An open book presentation of Fab492.1 (left) and Trx1 (right). Trx1 is rotated 180° around the vertical axis relative to Fab492.1. Residues from the light chain involved in interactions with Trx1 are white, interacting residues from CDR H3 are colored raspberry, and interacting residues from CDRs H2 and H1 are purple. Interacting residues from Trx1 are in corresponding colors.

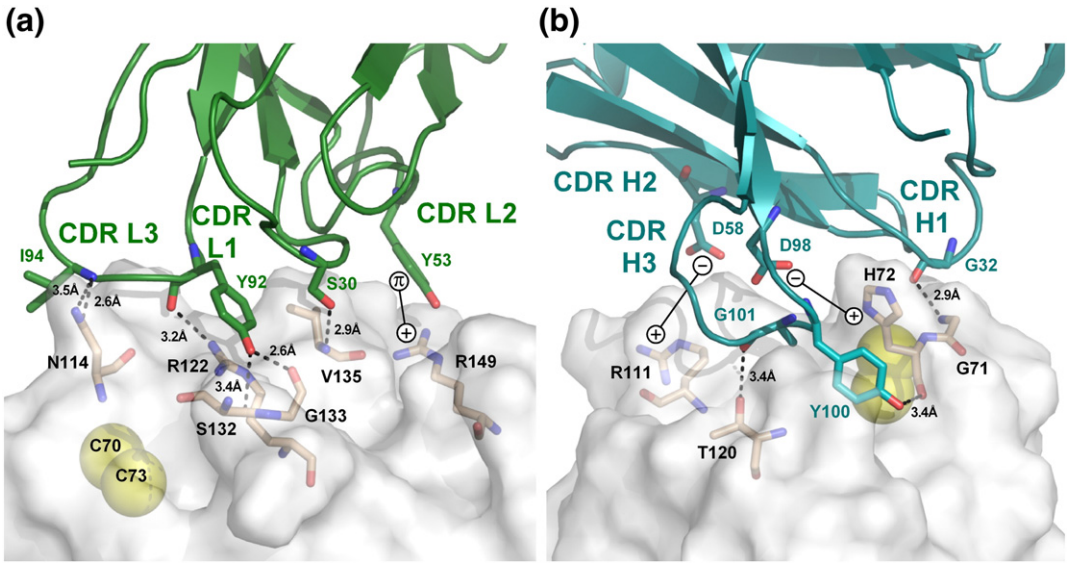

Fig. 6. Specific interactions between Trx1 residues and Fab492.1 residues. Fab492.1–HsQSOX1$_{Trx}$ interface residues between Trx1 and the light (a) and heavy (b) antibody chains are presented. Trx1 is shown in white surface representation, and interacting residues are shown as sticks labeled in black. The light chain (green) and heavy chain (blue) are shown in cartoon, and interacting residues are shown as sticks. CDRs are labeled. Hydrogen bonds are presented with black broken lines, and their distances are indicated. CXXC sulfurs are shown as spheres. Cation–π interactions and salt bridges are indicated. Additional Fab492.1–HsQSOX1$_{Trx}$ interactions are listed in Supplementary Table 1.

of unbound HsQSOX1$_{Trx}$, indicating that MAb492.1 blocks substrate access to the oxidoreductase active site without disrupting the HsQSOX1$_{Trx}$ structure. However, only one of the two conformations previously observed for the conserved tryptophan immediately upstream of the Trx1 CXXC motif in mammalian QSOX enzymes [16] is compatible with antibody binding.

Whereas MAb492.1 binds and blocks the redox-active site of the Trx1 domain, it does not appear to have any direct effect on the redox-active site of the FAD-binding domain, the seat of sulfhydryl oxidase activity in the enzyme. The two modules of HsQSOX1 are flexibly tethered to one another [16], and the antibody binding site on the HsQSOX1$_{Trx}$ module is far from the linker between the modules. The antibody is therefore not expected to interfere sterically with access of model substrates, in particular the small dithiol reagent DTT, to the FAD-proximal disulfide in the Erv domain. The dramatic effect of MAb492.1 on HsQSOX1 oxygen consumption, an event that occurs at the Erv domain, is thus most likely due to the failure of the antibody-bound Trx1 domain to supply electrons to the Erv domain, consistent with the proposed model for the QSOX1 mechanism [15,16].

Construction of a functional single-chain antibody fragment, scFv492.1

The variable regions that were identified from MAb492.1 were used to construct an scFv. The scFv is composed of the heavy-chain variable domain at the amino terminus, the light-chain variable domain at the carboxy terminus, and a linker of [Gly$_4$Ser]$_3$ connecting them. The nucleotide sequence encoding the scFv was optimized for translation in *Escherichia coli* and cloned into an expression vector introducing a His$_6$ tag at the amino terminus. The purified scFv, designated scFv492.1, was obtained from inclusion bodies after production in bacteria and was refolded to obtain functional material. Refolded scFv492.1 was tested in the colorimetric assay based on rdRNase oxidation and shown to inhibit 50 nM HsQSOX1 with an IC$_{50}$ of 250 ± 30 nM (Supplementary Fig. 6). A K_i of 130 ± 20 nM can be calculated directly from this IC$_{50}$ value [21], assuming that scFv492.1 is a competitive inhibitor. This assumption is valid since scFv492.1 is most likely to bind HsQSOX1 at the same site as MAb492.1, preventing substrate oxidation, but cannot be considered as a tight binding inhibitor because a fivefold excess is needed to inhibit HsQSOX1 under the same experimental conditions. Despite the difference in K_i between the MAb and the scFv, the latter is still a highly effective inhibitor. The successful construction of the single-chain antibody variant demonstrates that MAb492.1 activity can be recapitulated in recombinant constructs.

Discussion

In this study, we demonstrated that binding of antibody MAb492.1 to the redox-active site in the HsQSOX1 Trx1 domain blocks catalysis of disulfide

bond formation in model thiol substrates tested in *in vitro* enzyme assays. This finding supports the redox relay mechanism proposed for HsQSOX1, in which electrons enter the enzyme by dithiol/disulfide exchange at the Trx1 domain CXXC motif before being transferred to the site of sulfhydryl oxidase activity in the FAD-binding domain. Furthermore, we have shown that antibody binding to the Trx1 domain blocks HsQSOX1 activity on physiological substrates involved in ECM assembly and function. Thus, the HsQSOX1 relay mechanism is also relevant for the native extracellular activity of the enzyme.

The X-ray crystal structure of the complex between the Fab fragment of MAb492.1 and the target module of HsQSOX1 shows in detail how MAb492.1 occludes the Trx1 redox-active site of QSOX1. The antibody heavy-chain CDRs encircle the end of the Trx1 redox-active helix and are expected to thereby block both substrate access to the enzyme and formation of the enzyme conformation required for interdomain electron transfer [16]. Specifically, CDR H1 and CDR H3 provide tyrosine side chains that sandwich the conserved histidine in the Trx1 CXXC motif (CGHC), and the backbone carbonyl of a glycine residue in CDR H1 serves as a hydrogen bond acceptor for the exposed NH group of the CGHC glycine in Trx1. A large network of additional interactions supports the direct contacts of the antibody with the HsQSOX1 Trx1 redox-active site (Fig. 6). Notably, CDR H1 and CDR H3, which show the greatest structural divergence in MAb492.1 from the most common conformations in a catalog of antibody CDRs [30] (Supplementary Table 2), are the loops most deeply engaged with the topological and chemical features surrounding the HsQSOX1 active-site helix.

The tight-binding inhibitor of QSOX1 characterized structurally and mechanistically in this study is likely to find applications in basic research on ECM function, and perhaps eventually in the clinic due to the importance of ECM in various disease states. For example, the interactions between tumor cells and the surrounding stroma are critical for tumor cell survival and metastasis. Consequently, a number of the macromolecules that participate in these interactions are currently targeted or proposed as targets for cancer therapy. In particular, integrins, which mediate interactions between epithelial cells and the BM, offer one means of undermining stromal support of tumor cells [31,32]. In addition, laminin itself has been targeted for knockdown therapies [33], and blocking laminin receptors with antibodies has also been promoted [34]. The advantage of targeting HsQSOX1, which affects laminin incorporation into the ECM [5] and thereby the number of potential integrin interaction sites, is that HsQSOX1 mediates meshwork assembly enzymatically. Enzyme inhibition is amplified, due to the action of one enzyme on multiple substrate molecules, and therefore more potent than direct inhibition of protein-mediated adhesion.

Enzymes are powerful control points for regulation of biological systems in general and of ECM assembly in particular. However, it is thought that most ECM components spontaneously self-assemble, rather than requiring specific factors that catalyze their incorporation. Catalytic activities that introduce essential post-translational modifications to ECM proteins or their cell-surface scaffolds and thereby affect their assembly and binding properties usually occur inside the cell and cannot be accessed by antibody therapy. Furthermore, such modifications are often quite general and apply to numerous proteins, and thus the enzymes that catalyze them do not make useful drug targets. Examples of such modifications include hydroxylation of proline and N-linked glycosylation in the ER, as well as O-linked glycosylation in the Golgi apparatus. A more specific enzymatic modification introduced to a phosphorylated O-mannosyl glycan on the cell-surface protein dystroglycan promotes its function as a laminin docking site [35], but this reaction is sequestered in the Golgi and therefore not amenable to protein-drug treatment. Enzymes such as HsQSOX1 that act extracellularly to modulate the structure and properties of the ECM are rare and valuable targets.

Another enzyme that modulates ECM properties and can be accessed by extracellular agents is lysyl oxidase (LOX). Like HsQSOX1, LOX is up-regulated in many tumors [36], and inhibition of LOX has been shown to decrease tumor metastasis in mice [37]. LOX activity cross-links collagen and stiffens the ECM, which promotes integrin clustering, PI3 kinase activity, and, under pathological conditions, invasive cell behavior [38]. HsQSOX1 inhibition is highly complementary to LOX inhibition, because the two enzymes appear to affect complementary components (laminin *versus* collagen) of the BM with grossly similar outcomes. In contrast to LOX, however, HsQSOX1 does not appear to induce stiffening of ECM components that have already been incorporated into the matrix, but rather to influence ECM composition.

We report here the structural and functional characterization of a monoclonal antibody that inhibits HsQSOX1 in *in vitro* purified enzyme assays and in tissue culture assays that model tumor cell invasion of the stroma. We show that MAb492.1 is a highly effective, tight-binding inhibitor of HsQSOX1, and we use the antibody to demonstrate that the mechanism of QSOX1 activity on model thiol substrates *in vitro* and on native substrates in fibroblast ECM appears to be similar. The favorable properties of MAb492.1 suggest that this monoclonal antibody will be an excellent starting point for humanization and the generation of recombinant variants optimized for therapeutic applications.

Materials and Methods

Plasmid construction

ScFv and HsQSOX1 synthetic genes codon optimized for protein production in *E. coli* (Genescript) were cloned between the NdeI and BamHI sites of the pET-15b vector (Novagen). The amino-terminal and carboxy-terminal HsQSOX1 fragment construction was previously described [16].

Expression and purification of proteins

Codon-optimized HsQSOX1 was expressed and purified essentially as described for a previous HsQSOX1 construct [16], except that the amino-terminal His_6 tag was removed after purification on a Ni-NTA column (GE Healthcare). The eluted enzyme was exchanged into 20 mM sodium phosphate buffer, pH 7.4, 100 mM NaCl, and 20 mM imidazole using a PD-10 desalting column (GE Healthcare). Thrombin (10 U/mg protein) was added, and the cleavage reaction was allowed to proceed overnight at room temperature (RT). PMSF was added to 1 mM to inhibit the thrombin, and the protein was re-applied to a Ni-NTA column. Further purification was performed by size-exclusion chromatography in 20 mM sodium phosphate buffer, pH 7.5, 200 mM NaCl, and 0.5 mM ethylenediaminetetraacetic acid (EDTA).

The amino-terminal and carboxy-terminal HsQSOX1 fragments were expressed and purified as previously described [16,28].

Monoclonal antibody MAb492.1 was produced and purified as previously described [5].

HsQSOX1 inhibition assay

Reactions of 100 µL volume were conducted in 96-well plates (Nunc). rdRNase was used as a model substrate and was prepared as follows. Ten milligrams of RNase A (Sigma) was dissolved in 1 mL of 20 mM phosphate buffer, pH 6.5, 6 M GuHCl, and 100 mM DTT, and incubated at 37 °C for 1 h. The protein was desalted on a PD-10 column (GE Healthcare) equilibrated with H_2O, and its thiol content was determined by 5,5′-dithiobis-(2-nitrobenzoic acid) (DTNB) absorbance at 412 nm. Fifty nanomolar HsQSOX1, unless otherwise noted, was incubated with various concentrations of MAb492.1, Fab492.1, or scFv492.1 for 30 min at RT. Reactions were initiated with the addition of 200 µM RNase thiols and were quenched after 25 min with 1 mM DTNB. Absorbance was measured at 405 nm in a microplate reader. Measurements were repeated three times for each MAb492.1 concentration. Data were fit using a sigmoidal function with four parameters:

$$y = \min + \frac{(\max - \min)}{1 + 10^{\mathrm{Hill}(\log(IC_{50}) - x)}}$$

where min and max are the lower and upper asymptotes of the curve, Hill is the slope of the curve at its midpoint, and IC_{50} is the concentration of antibody in which the activity of HsQSOX1 is reduced by 50%. All data fitting was done using Origin.

ELISA binding assay

A 96-well plate (Nunc) was coated with 100 µL of HsQSOX1 or one of its fragments at various concentrations, or 5% bovine serum albumin (BSA) in phosphate-buffered saline (PBS) containing 0.1% Tween (PBS-T) as a control, for 1 h at 37 °C. The wells were blocked with 5% BSA in PBS-T at RT for 1 h. MAb492.1 was then added to the wells for 1 h at RT, followed by three washes with 300 µL of PBS-T. Polyclonal goat anti-mouse antibody conjugated to horseradish peroxidase in 5% BSA was added at a 1:2500 dilution and incubated at RT for 30 min. Wells were washed three times with 300 µL of PBS-T and 100 µL of 3,3′,5,5′-tetramethylbenzidine (Millipore) was added. Absorbance was read at 630 nm in a microplate reader (TECAN).

Inhibitory constant determination

A Clarke-type oxygen electrode (Hansatech Instruments) was used to monitor changes in dissolved oxygen concentration as a measure of HsQSOX1 activity. Twenty-five nanomolar HsQSOX1 and various concentrations (1–250 nM) of purified MAb492.1 were assayed in 50 mM potassium phosphate buffer, pH 7.5, 65 mM NaCl, and 1 mM EDTA. Reactions were started by injection of DTT to a concentration of 200 µM in the electrode reaction chamber. Three independent progress curves were collected for each MAb492.1 concentration, and initial slopes were calculated. The background decrease in oxygen concentration due to the presence of DTT and MAb492.1 was measured and subtracted from the initial slopes to obtain the rates of HsQSOX1 activity in the presence of various concentrations of MAb492.1. The ratios of the initial rates of HsQSOX1 in the presence and absence of inhibitor were plotted as a function of inhibitor concentration. The data were fit to the following equation [20,21] for obtaining K_i for a tight binding inhibitor:

$$\frac{v_i}{v_0} = \frac{1}{2[E_0]}\left(([E_0] - [I_0] - K_i) + \sqrt{(I_0 + K_i - [E_0])^2 + 4K_i[E_0]}\right)$$

where v_0 is the velocity of reaction in the absence of MAb492.1, v_i is the velocity in the presence of MAb492.1, $[E_0]$ is the total enzyme concentration (25 nM), $[I_0]$ is the total MAb492.1 concentration, and K_i is the inhibitory constant to be determined.

The K_i of scFv492.1 was calculated from the IC_{50} value obtained by the colorimetric assay based on rdRNase oxidation, using the equation for classical competitive inhibition [21]: $K_i = IC_{50}/(1 + [S]_0/K_m)$, where $[S]_0$ is the initial substrate concentration and K_m is the Michaelis constant of HsQSOX1 for rdRNase, which is 320 ± 35 µM [15].

Cell adhesion and migration assays

Cell adhesion and migration assays were conducted essentially as previously described [5]. In both assays, fibroblasts were grown for 4 days in the presence of various concentrations of MAb492.1 before the medium was exchanged and fluorescently labeled epithelial cells were added. Experiments were performed in triplicate and quantified by counting cells from seven 10× fields for each sample.

Variable region sequencing

Total RNA was extracted from ~11 × 10^6 anti-MAb492.1 hybridoma cells using the RNeasy mini kit (Qiagen). Five hundred nanograms of total RNA was reverse transcribed into first-strand cDNA by using polydT primer and 20 U of Moloney murine leukemia virus reverse transcriptase. The variable region of the light chain was amplified using degenerate primers [23], and the variable region of the heavy chain was amplified using optimized primers for mouse scFv repertoire cloning [24]. PCR products of ~300 bp were gel extracted with the HiYield Gel/PCR DNA fragments extraction kit (RBCBioscience) and cloned into pGEM-T easy vector (Promega). The inserts were sequenced using T7 and SP6 primers and analyzed with the aid of the ImMunoGeneTics database. For verification of sequences by LC–MS/MS, Mab492.1 was treated with DTT, and the heavy and light chains were separated by SDS-PAGE. Coomassie-stained bands were digested in-gel with trypsin or a combination of chymotrypsin and Asp-N proteases. Protease cleavage, gel extraction, and LC–MS/MS were performed as previously described [16].

Analytical size-exclusion chromatography

One hundred microliters of 20 μM HsQSOX1, its fragments, or MAb492.1 was loaded onto a Superdex 200 column (GE HealthCare) equilibrated with 20 mM sodium phosphate buffer, pH 7.4, 200 mM NaCl, and 1 mM EDTA at a flow rate of 0.8 mL/min. The complexes (200 μL) of HsQSOX1, or its fragments, with MAb492.1 were injected after 30 min co-incubation at RT.

Fab492.1–HsQSOX1$_{Trx}$ complex purification and crystallization

Purified MAb492.1 concentrated to 1.5 mg/mL in PBS was digested at 37 °C with papain (Sigma) at a 1:20 papain:MAb492.1 ratio. Prior to use, papain was activated by dissolving in PBS supplemented with 20 mM EDTA and 20 mM cysteine. Digestion was stopped after 4 h using leupeptin, and the digested antibody was dialyzed against PBS, pH 8. The Fab fragment of MAb492.1 was purified by size-exclusion chromatography followed by protein G. Purified Fab492.1 was incubated for 1 h at 4 °C with a twofold excess of HsQSOX1$_{Trx}$, and the complex was isolated by size-exclusion chromatography in 10 mM Tris, pH 7.5, and 100 mM NaCl. The complex was concentrated using a centrifugal concentrator to 11 mg/mL. Crystals were grown by hanging-drop vapor diffusion at 293 K by mixing 1 μL of protein complex solution with 1 μL of well solution (19% w/v polyethylene glycol 4 kDa and 0.4 M ammonium phosphate dibasic) and suspending over well solution. Crystals were transferred to a solution containing 20% w/v polyethylene glycol 4 kDa, 25% glycerol, and 0.35 M ammonium phosphate dibasic and flash frozen in a nitrogen stream at 100 K.

Data collection

Diffraction data were collected at 100 K on a RU-H3R generator (Rigaku) equipped with a RaxisIV++ image plate system and Osmic mirrors. Data were collected to 2.7 Å resolution from a crystal of space group $P6_1$ with unit cell dimensions $a = b = 209.31$ Å, $c = 55.27$ Å, $\alpha = \beta = 90°$, and $\gamma = 120°$ Data were processed and scaled using DENZO and SCALEPACK [39].

Structure solution

The Fab492.1–HsQSOX1$_{Trx}$ complex structure was determined by molecular replacement using Phaser [40]. First, the structure of HsQSOX$_{Trx}$ [16] was used for the search, and suitable rotation and translation solutions were found. Then, the constant region of a Fab structure with 75% sequence identity [Protein Data Bank (PDB) code: 3OKD] was used as a search model, and finally the variable region without the CDR loops from the same Fab model was searched. Refinement was performed using CNS [41], and addition of CDR loops and model rebuilding were done using Coot [42]. Validation of the structures was performed using MolProbity [43], according to which there were no Ramachandran outliers and the structure model was rated in the top 95% in its resolution range.

ScFv expression, purification, and refolding

ScFv492.1 was produced in the BL21 (DE3) plysS *E. coli* strain grown in LB medium supplemented with 100 μg/mL ampicillin and 30 μg/mL chloramphenicol. Transformed cells were grown at 37 °C, and induction was carried out by addition of isopropyl-β-D-1-thiogalactopyranoside to a concentration of 0.5 mM when cells reached an optical density of 0.5 at 595 nm. After induction, cells were grown overnight at 25 °C. Cells were harvested by centrifugation for 30 min at 4000 rpm. Cell pellets were suspended in 20 mM sodium phosphate buffer, pH 7.4, 500 mM NaCl, and 20 mM imidazole, supplemented with protease inhibitors. The cell lysate was centrifuged at 40,000***g*** for 1 h. Pellets were dissolved in 50 mM Tris buffer, pH 8, 100 mM NaCl, 1 mM EDTA, and 0.5% Triton X-100; sonicated three times for 30 s; and centrifuged again for 10 min. The supernatant was discarded, and the sonication and centrifugation procedure was repeated three times, the last time without Triton X-100. Pellets were dissolved in 50 mM Tris buffer, pH 7.8, 6 M GuHCl, and 10 mM β-mercaptoethanol at 4 °C overnight. The dissolved scFv was purified on a Ni-NTA column in denaturing conditions (6 M GuHCl), eluting with a pH gradient between pH 6.9 and pH 3.8. Refolding was performed as previously described [44].

PDB accession code

The coordinates and structure factors have been deposited with PDB code 4IJ3.

Acknowledgements

The authors are grateful to Y. Yarden for advice and support. The authors acknowledge O. Leitner, Z.

Landau, and H. Hamawi from the Weizmann Institute Antibody Unit for performing all technical aspects of antibody elicitation and production. E. Wong, Y. Udi, and A. Trahtenhercts provided advice on antibody sequencing. N. Sela assisted with antibody isotyping. This research was supported by the Israel Science Foundation, the Israel Cancer Association, and the European Research Council under the European Union's Seventh Framework Programme (ERC Grant agreement number 310649).

Supplementary Data

Supplementary data to this article can be found online at http://dx.doi.org/10.1016/j.jmb.2013.07.011

Received 3 June 2013;
Accepted 9 July 2013
Available online 15 July 2013

Keywords:
monoclonal antibody;
anti-metastatic drugs;
disulfide bonds;
laminin;
extracellular matrix

Abbreviations used:
QSOX1, quiescin sulfhydryl oxidase 1; FAD, flavin adenine dinucleotide; ER, endoplasmic reticulum; BM, basement membrane; ECM, extracellular matrix; Trx, thioredoxin-fold; Erv, Erv-fold; HsQSOX1, recombinant human QSOX1; rdRNase, reduced and denatured RNase A; DTNB, 5,5′-dithiobis-(2-nitrobenzoic acid); LC–MS/MS, liquid chromatography–tandem mass spectrometry; scFv, single-chain variable fragment; CDR, complementarity-determining region; LOX, lysyl oxidase; EDTA, ethylenediaminetetraacetic acid; PEG, polyethylene glycol; PBS, phosphate-buffered saline; PBS-T, PBS with 0.1% Tween; HRP, horseradish peroxidase; BSA, bovine serum albumin; RT, room temperature; PDB, Protein Data Bank.

References

[1] Hoober KL, Joneja B, White III HB, Thorpe C. A sulfhydryl oxidase from chicken egg white. J Biol Chem 1996;271: 30510–6.
[2] Bulleid NJ, Ellgaard L. Multiple ways to make disulfides. Trends Biochem Sci 2011;36:485–92.
[3] Mesecke N, Terziyska N, Kozany C, Baumann F, Neupert W, Hell K, et al. A disulfide relay system in the intermembrane space of mitochondria that mediates protein import. Cell 2005;121:1059–69.
[4] Coppock D, Kopman C, Gudas J, Cina-Poppe DA. Regulation of the quiescence-induced genes: quiescin Q6, decorin, and ribosomal protein S29. Biochem Biophys Res Commun 2000;269:604–10.
[5] Ilani T, Alon A, Grossman I, Horowitz B, Kartvelishvily E, Cohen S, Fass D. A secreted disulfide catalyst controls extracellular composition and function. Science 2013;341: 74–6.
[6] Yurchenco PD. Basement membranes: cell scaffoldings and signaling platforms. Cold Spring Harbor Perspect Biol 2011;3:1–20.
[7] Spessotto P, Gronkowska A, Deutzmann R, Perris R, Colombatti A. Preferential locomotion of leukemic cells toward laminin isoforms 8 and 10. Matrix Biol 2003;4:351–61.
[8] Ljubimova JY, Fujita M, Khazenzon NM, Ljubimova AV, Black KL. Changes in laminin isoforms associated with brain tumor invasion and angiogenesis. Front Biosci 2006;11:81–8.
[9] Huang X, Ji G, Wu Y, Wan B, Yu L. LAMA4, highly expressed in human hepatocellular carcinoma from Chinese patients, is a marker of tumor invasion and metastasis. J Cancer Res Clin Oncol 2008;134:705–14.
[10] Nagato S, Nakagawa K, Harada H, Kohno S, Fujiwara H, Sekiguchi K, et al. Downregulation of laminin α4 chain expression inhibits glioma invasion in vitro and in vivo. Int J Cancer 2005;117:41–50.
[11] Zhao W, Han HB, Zhang ZQ. Suppression of lung cancer cell invasion and metastasis by connexin43 involves the secretion of follistatin-like 1 mediated via histone acetylation. Int J Biochem Cell Biol 2011;43:1459–68.
[12] Modlich O, Prisack HB, Pitschke G, Ramp U, Ackermann R, Bojar H, et al. Identifying superficial, muscle-invasive, and metastasizing transitional cell carcinoma of the bladder: use of cDNA array analysis of gene expression profiles. Clin Cancer Res 2004;10:3410–21.
[13] Beroukhim R, Brunet JP, Di Napoli A, Mertz KD, Seeley A, Pires MM, et al. Patterns of gene expression and copy-number alterations in von-Hippel Lindau disease-associated and sporadic clear cell carcinoma of the kidney. Cancer Res 2009;69:4674–81.
[14] Badea L, Herlea V, Dima SO, Dumitrascu T, Popescu I. Combined gene expression analysis of whole-tissue and microdissected pancreatic ductal adenocarcinoma identifies genes specifically overexpressed in tumor epithelia. Hepatogastroenterology 2008;55:2016–27.
[15] Heckler EJ, Alon A, Fass D, Thorpe C. Human quiescin-sulfhydryl oxidase, QSOX1: probing internal redox steps by mutagenesis. Biochemistry 2008;47:4955–63.
[16] Alon A, Grossman I, Gat Y, Kodali VK, DiMaio F, Mehlman T, et al. The dynamic disulfide relay of quiescin sulfhydryl oxidase. Nature 2012;488:414–8.
[17] Altshuler EP, Serebryanaya DV, Katrukha AG. Generation of recombinant antibodies and means for improving their affinity. Biochemistry 2010;75:1584–605.
[18] Weiner LM, Surana R, Wang S. Monoclonal antibodies: versatile platforms for cancer immunotherapy. Nat Rev Immunol 2010;10:317–27.
[19] Maynard J, Georgiou G. Antibody engineering. Annu Rev Biomed Eng 2000;2:339–76.
[20] Morrison JF. Kinetics of the reversible inhibition of enzyme-catalyzed reactions by tight-binding inhibitors. Biophys Biochim Acta 1969;185:269–86.
[21] Bieth JG. Theoretical and practical aspects of proteinase inhibition kinetics. Methods Enzymol 1995;248: 59–84.
[22] Seymour JL, Lindquist RN, Dennis SM, Moffat B, Yansura D, Reilly D, et al. Ecotin is a potent anticoagulant and reversible tight-binding inhibitor of factor Xa. Biochemistry 1994;33: 3949–58.
[23] Benhar I, Reiter Y. Phage display of single-chain antibody constructs. Curr Protoc Immunol 2002;48: 10.19B.1–10.19B.31.

[24] Wang Y, Chen W, Li X, Cheng B. Degenerated primer design to amplify the heavy chain variable region from immunoglobulin cDNA. BMC Bioinformatics 2006;7:s9.
[25] Zhou H, Fisher RJ, Papasll TS. Optimization of primer sequences for mouse scFv repertoire display library construction. Nucleic Acids Res 1994;22:888–9.
[26] Lefranc MP, Giudicelli V, Kaas Q, Duprat E, Jabado-Michaloud J, Scaviner D, et al. IMGT, the international ImMunoGeneTics information system. Nucleic Acids Res 2004;33:593–7.
[27] Raje S, Thorpe C. Inter-domain redox communication in flavoenzymes of the quiescin/sulfhydryl oxidase family: role of a thioredoxin domain in disulfide bond formation. Biochemistry 2003;42:4560–8.
[28] Alon A, Heckler EJ, Thorpe C, Fass D. QSOX contains a pseudo-dimer of functional and degenerate sulfhydryl oxidase domains. FEBS Lett 2010;584:1521–5.
[29] Mitra P, Pal D. New measures for estimating surface complementarity and packing and protein–protein interfaces. FEBS Lett 2010;584:1163–8.
[30] North B, Lehmann A, Dunbrack Jr RL. A new clustering of antibody CDR loop conformations. J Mol Biol 2011;406:228–56.
[31] Sawada K, Mitra AK, Radjabi AR, Bhaskar V, Kistner EO, Tretiakova M, et al. Loss of E-cadherin promotes ovarian cancer metastasis via α5-integrin, which is a therapeautic target. Cancer Res 2008;68:2329–39.
[32] Weaver VM, Petersen OW, Wang F, Larabell CA, Briand P, Damsky C, et al. Reversion of the malignant phenotype of human breast cells in three-dimensional culture and in vivo by integrin blocking antibodies. J Cell Biol 1997;137:231–45.
[33] Fujita M, Lee BS, Khazenzon NM, Penichet ML, Wawrowsky KA, Patil R, et al. Brain tumor tandem targeting using a combination of monoclonal antibodies attached to biopoly(beta-L-malic acid). J Control Release 2007;122:356–63.
[34] Omar A, Reusch U, Knackmuss S, Little M, Weiss SF. Anti-LRP/LR-specific antibody IgG1-iS18 significantly reduces adhesion and invasion of metastatic lung, cervix, colon and prostate cancer cells. J Mol Biol 2012;419:102–9.
[35] Inamori K, Yoshida-Moriguchi T, Hara Y, Anderson ME, Yu L, Campbell KP. Dystroglycan function requires xylosyl- and glucoronyltransferase activities of LARGE. Science 2012;335:93–6.
[36] Erler JT, Bennewith KL, Cox TR, Lang G, Bird D, Koong A, et al. Hypoxia-induced lysyl oxidase is a critical mediator of bone marrow cell recruitment to form the premetastatic niche. Cancer Cell 2009;15:35–44.
[37] Erler JT, Giaccia AJ. Lysyl oxidase mediates hypoxic control of metastasis. Cancer Res 2006;66:10238–41.
[38] Levental KR, Yu H, Kass L, Lakins JN, Egeblad M, Erler JT, et al. Matrix crosslinking forces tumor progression by enhancing integrin signaling. Cell 2009;139:891–906.
[39] Otwinowski Z, Minor W. Processing of X-ray diffraction data collected in oscillation mode. Methods Enzymol 1997;276:307–26.
[40] McCoy AJ, Grosse-Kunstleve RW, Adams PD, Winn MD, Storoni LC, Read RJ. Phaser crystallographic software. J Appl Crystallogr 2007;40:658–74.
[41] Brunger AT, Adams PD, Clore GM, DeLano WL, Gross P, Grosse-Kunstleve RW, et al. Crystallography & NMR system: a new software suite for macromolecular structure determination. Acta Crystallogr Sect D 1998;54:905–21.
[42] Emsley P, Cowtan K. Coot: model-building tools for molecular graphics. Acta Crystallogr Sect D 2005;60:2126–32.
[43] Lovell SC, Davis IW, Arendall III WB, de Bakker PI, Word JM, Prisant MG, et al. Structure validation by Cα geometry: φ, ψ and Cβ deviation. Proteins 2003;50(3):437–50.
[44] Kouhei T, Katsutoshi S, Hidemasa K, Makoto U, Takeo J, Izumi K. Highly efficient recovery of functional single-chain Fv fragments from inclusion bodies overexpressed in *Escherichia coli* by controlled introduction of oxidizing reagent—application to a human single-chain Fv fragment. J Immunol Methods 1998;219:119–29.